An Incompressible Log-Domain Demons Algorithm for Tracking Heart Tissue

K. McLeod[1], A. Prakosa[1], T. Mansi[2], M. Sermesant[1], and X. Pennec[1]

[1] INRIA Méditerranée, Asclepios Project, Sophia Antipolis, France
[2] Siemens Corporate Research, Image Analytics and Informatics, Princeton, NJ, U.S.A

Abstract. We describe an application of the previously proposed iLogDemons algorithm to the STACOM motion-tracking challenge data. The iLogDemons algorithm is a consistent and efficient framework for tracking left-ventricle heart tissue using an elastic incompressible non-linear registration algorithm based on the LogDemons algorithm. This method has shown promising results when applied to previous data-sets. Along with having the advantages of the LogDemons algorithm such as computing deformations that are invertible with smooth inverse, the method has the added advantage of allowing physiological constraints to be added to the deformation model. The registration is entirely performed in the log-domain with the incompressibility constraint strongly ensured and applied directly in the demons minimisation space. Strong incompressibility is ensured by constraining the stationary velocity fields that parameterise the transformations to be divergence-free in the myocardium. The method is applied to a data-set of 15 volunteers and one phantom, each with echocardiography, cine-MR and tagged-MR images. We are able to obtain reasonable results for each modality and good results for echocardiography images with respect to quality of the registration and computed strain curves.

1 Methodology

1.1 Cardiac Motion Tracking using Physiological Constraints

Tracking cardiac motion from 3D images is a difficult task due to the complex movement of the myocardium through the cardiac cycle. The left ventricular (LV) movement includes a contraction of the ventricle with a longitudinal motion towards the apex as well as a twisting motion from the base of the ventricle in the circumferential direction. Common methods for motion tracking using non-rigid registration are able to capture the dilation of the ventricle, however capturing the twisting motion is a difficult task. The incompressible log-domain demons algorithm described in [1] (iLogDemons for short) aims to tackle this problem by imposing physiological constraints (such as incompressibility and elasticity in the myocardium) in the previously proposed log-domain demons algorithm (LogDemons) [2]. For the purpose of this work we don't provide here a state of the art on cardiac motion tracking algorithms, but rather refer the reader to [1]

and references therein. We apply the iLogDemons method to a 3D data-set of 15 volunteers and one phantom with echocardiography, cine-MR and tagged-MR image sequences. The method is described here in brief, for a more thorough and descriptive analysis see [1].

1.2 Review of the Log-Domain Demons Algorithm

The iLogDemons algorithm is an extension of the LogDemons algorithm [2]. The LogDemons algorithm estimates a dense non-linear transformation ϕ that best aligns a template image T to a reference image R. The transformation ϕ is parameterised by stationary velocity fields $\mathbf{v}$ through the exponential map $\phi = \exp(\mathbf{v})$ [3]. The images R and T are registered by minimising in the space of velocities (the log-domain) the energy functional: $\varepsilon(\mathbf{v}, \mathbf{v}_c) = 1/\sigma_i^2 \parallel R - T \circ \exp(\mathbf{v}_c) \parallel_{L_2}^2 + 1/\sigma_x^2 \parallel \log(\exp(-\mathbf{v}) \circ \exp(\mathbf{v}_c)) \parallel_{L_2}^2 + 1/\sigma_d^2 \parallel \nabla \mathbf{v} \parallel^2$, where σ_i^2 relates to the noise in the images and σ_d^2 controls the regularisation strength. The velocity field $\mathbf{v}$ parameterises the transformation ϕ, and $\mathbf{v}_c$ parameterises an intermediate transformation $\phi_c = \exp(\mathbf{v}_c)$ that models the *correspondences* between the voxels of the two images. During the *optimisation step*, $\varepsilon(\mathbf{v}, \mathbf{v}_c)$ is minimised with respect to $\mathbf{v}_c$. Under the diffeomorphic update rule $\phi_c \leftarrow \phi \circ \exp(\delta\mathbf{v})$, the optimal update velocity writes $\delta\mathbf{v}(\mathbf{x}) = (R(\mathbf{x}) - T \circ \phi(\mathbf{x}))/(\parallel (J(\mathbf{x}) \parallel^2 + \sigma_i/\sigma(\mathbf{x}))J(\mathbf{x})$. In this equation, $J(\mathbf{x})$ is the symmetric gradient $J(\mathbf{x}) = (\nabla R(\mathbf{x}) + \nabla(T \circ \phi)(\mathbf{x}))/2$. The correspondence velocity $\mathbf{v}_c$ is then updated using the first order approximation of the Baker-Campbell-Hausdorff (BCH) formula $\mathbf{v}_c = Z(\mathbf{v}, \delta\mathbf{v}) = \mathbf{v} + \delta\mathbf{v} + 1/2[\mathbf{v}, \delta\mathbf{v}] + 1/12[\mathbf{v}, [\mathbf{v}, \delta\mathbf{v}]] + O(\parallel \delta\mathbf{v} \parallel^2)$, where the Lie bracket $[\cdot, \cdot]$ is defined by $[\mathbf{v}, \delta\mathbf{v}] = (\nabla\mathbf{v})\delta\mathbf{v} - (\nabla\delta\mathbf{v})\mathbf{v}$. Finally, the *regularisation step* estimates the optimal regularised transformation ϕ by minimising $\varepsilon(\mathbf{v}, \mathbf{v}_c)$ with respect to $\mathbf{v}$, which is approximated by smoothing the correspondence velocity $\mathbf{v}_c$ with a Gaussian kernel G_σ.

1.3 Modeling Elasticity in the Myocardium

In order to incorporate an elastic regularizer into the LogDemons framework, a consistent mathematical formulation of the LogDemons regularisation is required. In [1] a closed-form expression of the demons Gaussian regulariser $\varepsilon_{reg}(\mathbf{v}) = 1/\sigma_x^2 \parallel \log(\exp(-\mathbf{v}) \circ \exp(\mathbf{v}_c)) \parallel_{L_2}^2 + 1/\sigma_d^2 \parallel \nabla\mathbf{v} \parallel^2$ is given by linearising the first term using the BCH formula and replacing the second term with the infinite sum Tikhonov regulariser. We could then replace the Gaussian regularizer by an elastic-like one, in a consistent way. The proposed elastic regularizer amounts to filtering the correspondence velocities by the elastic-like kernel:

$$\mathbf{v} = \left(G_\sigma Id + \frac{\sigma^2\kappa}{1+\kappa} HG_\sigma \right) \star \mathbf{v}_c = G_{\sigma,\kappa} \star \mathbf{v}_c \tag{1}$$

where $\sigma^2 = 2/\sigma_d^2$, HG_σ is the Hessian of the Gaussian kernel G_σ and $G_{\sigma,\kappa}$ is the elastic-like vector filter. In this formulation, $\kappa > 0$ penalises the global compressibility, and setting $\kappa = 0$ gives the Gaussian filter used in the LogDemons algorithm.

1.4 Incorporating Strong Incompressibility in the Myocardium

Incorporating incompressibility into the LogDemons consists in constraining the velocity fields $\mathbf{v}$ to be divergence-free. Demons optimisation step is not modified, as it optimises $\mathbf{v}_c$ only, but demons regularisation energy is now optimised under the divergence-free constraint, which amounts to minimising the Lagrange function:

$$P(\mathbf{v}, p) = \frac{1}{\sigma_x^2} \parallel \mathbf{v}_c - \mathbf{v} \parallel_{L_2}^2 + \int_\Omega \sum_{k=1}^{+\infty} \frac{Q_{el}^k(\mathbf{v})}{\sigma_x^2 \sigma_d^{2k}} - \frac{2}{\sigma_x^2} \int_\Omega p \nabla \cdot \mathbf{v}. \tag{2}$$

where Q_{el}^k is the k^{th} order isotropic differential quadratic form (IDQF) of a vector field $\mathbf{v}$ defined by $Q_{el}^k(\mathbf{v}) = \alpha_k \delta_{i_1 \ldots i_k} \mathbf{v}_{i_{k+1}} \delta_{i_1 \ldots i_k} \mathbf{v}_{i_{k+1}} + \beta_k \delta_{i_1 \ldots i_k} \mathbf{v}_{i_{k+1}} \delta_{i_2 \ldots i_k} \mathbf{v}_{i_1}$. In this equation, the Lagrange multiplier p is a scalar function of the Sobolev space $H_0^1(\Omega)$ that vanishes at infinity. The second term is the elastic-like regularizer that leads to the filter previously mentioned. We refer the reader to [1] for details.

Optima of (2) are found by solving $\delta_{\mathbf{v}} P(\mathbf{v}, p) = 0$:

$$\mathbf{v} + \sum_{k=1}^{\infty} \frac{(-1)^k}{\sigma_d^{2k}} (\alpha_k \Delta^k \mathbf{v} + \beta_k \Delta^{k-1} \nabla \nabla^T \mathbf{v}) = \mathbf{v}_c - \nabla p \tag{3}$$

with $p = 0$ at the domain boundaries $\delta\Omega$. The divergence of (3) under the optimal condition $\nabla \cdot v = 0$ yields the Poisson equation $\Delta p = \nabla \cdot \mathbf{v}_c$ with 0-Dirichlet boundary conditions, which can be solved independently of $\mathbf{v}$ to get p. The right hand side of (3) is thus the L_2 projection of $\mathbf{v}_c$ onto the space of divergence-free vector fields. Computationally, the divergence-free constraint on the velocity fields is enforced by smoothing the velocity field then projecting onto the space of divergence-free velocity fields. This is theoretically the same as projecting onto the space of divergence-free velocity fields then smoothing the results since convolution and derivatives commute (up to issues at the boundary).

Algorithm 1 summarises the main steps of the method. Implementation of this algorithm is described in the following section. A more thorough description of the derivations of the previous equations can be found in [1].

Algorithm 1 iLogDemons: Incompressible Elastic LogDemons Registration

Require: Stationary velocity field $\mathbf{v}^0$. Usually $\mathbf{v}^0 = \mathbf{0}$ i.e. $\phi^0 = Id$.

1: **loop** {*over n until convergence*}
2: Compute the update velocity: $\delta\mathbf{v}^n$ (see [1]).
3: Fluid-like regularisation: $\delta\mathbf{v}^n \leftarrow G_{\sigma_f} \star \delta\mathbf{v}^n$, G_{σ_f} is a Gaussian kernel.
4: Update the correspondence velocity: $\mathbf{v}^n \leftarrow Z(\mathbf{v}^{n-1}, \delta\mathbf{v}^n)$ (see [2]).
5: Elastic-like regularisation: $\mathbf{v}^n \leftarrow G_{\sigma,\kappa} \star \mathbf{v}^n$ (see [1]).
6: Solve: $\Delta p = \nabla \cdot \mathbf{v}^n$ with 0-Dirichlet boundary conditions.
7: Project the velocity field: $\mathbf{v}^n \leftarrow \mathbf{v}^n - \nabla p$.
8: Update the warped image $T \circ \phi^n = T \circ \exp(\mathbf{v}^n)$.
9: **return** $\mathbf{v}$, $\phi = \exp(\mathbf{v})$ and $\phi^{-1} = \exp(-\mathbf{v})$.

2 Implementation

The algorithm has been implemented using ITK and the open source implementation of the LogDemons algorithm [4]. The Poisson equation (which is solved at the incompressible domain) is discretised on the image grid using finite difference schemes [5] as the incompressible domain Γ may be of irregular shape. Image gradients are computed with periodic boundary conditions over the entire image domain [4] and the Gaussian filters are implemented with ITK recursive filters.

Despite the additional constraints, the complexity of the algorithm remains reasonable with respect to the LogDemons algorithm. Demons update velocity is computed at each voxel. The elastic-like filter is computed using Gaussian convolutions, therefore no significant overhead is added to the original Gaussian filtering. The complexity of the divergence-free projector directly depends on the number of voxels of the incompressible domain Γ.

The algorithm requires computing i) the divergence of the velocity field, ii) the gradient of the pressure field p, and iii) solving a linear system with $n \times n$ elements, where n is the number of voxels of the incompressible domain. The divergence and gradient operators are linear in the number of voxels. The Poisson Equation is solved at each iteration using iterative solvers like GMRES [6].

The codes are written in C++ and require as input the fixed image file and moving image file, as well as optional input of the mask image file, and registration parameters. The parameters used in the registration are summarized in the table below. These values were chosen based on tests performed on similar data-sets that concluded that the key parameter of interest is σ, which defines the weight of the Gaussian smoothing of the velocity field (in mm). The original voxel size of the images are$0.67 \times 0.68 \times 0.58$ for echocardiography, $1.25 \times 1.25 \times 8$ for cine-MR and $0.96 \times 0.96 \times 0.96$ for tagged-MR. The choice of σ is generally based on the voxel size to be around 1-2 times the largest original voxel size. Given the large difference in voxel size for cine-MR σ was a trade-off between the largest and smallest voxel size. More levels were used for the echocardiography sequences to speed up convergence of the simulation. This could also be done for the cine-MR sequences but was not considered necessary in this case. For the tagged-MR sequences, increasing the number of multi-resolution levels can remove the tags from under-sampling.

3 Image Pre-Processing

In order to apply the algorithm to the different data types, some pre-processing is needed to prepare the data. The method is defined in a way such that the user can give as input a region (which we define as a binary image with value 1 in the incompressible region and value 0 outside) where the incompressibility constraint is imposed. This region is defined at one time-frame only (end diastole). If no input is given the entire image is constrained to be incompressible, otherwise the user can turn off the incompressibility constraint (giving the standard

Input parameters:	Echo	Cine	Tag
Multi-resolution levels (frame-by-frame registration)	3	2	2
Multi-resolution levels (refinement step)	2	1	1
Number of iterations / level	100	100	100
Sigma (update field) in *mm*	0.5	0.5	0.5
Kappa (update field) in *mm*	0	0	0
Sigma (stationary velocity field) in *mm*	0.5	2	2
Kappa (stationary velocity field) in *mm*	1	1	1
Incompressibility update field (0-Disable,1-Enable)	0	0	0
Incompressibility velocity field (0-Disable,1-Enable)	1	1	1

LogDemons algorithm). Therefore, in order to use the iLogDemons algorithm, we need to define the region where we impose the incompressibility constraint by delineating the left ventricle myocardium using image segmentation tools (since in this case we are interested in the deformation of the left ventricle). Note that for the cine-MR sequences we segmented also the right ventricle since it is clearly visible in all the images and provides added information to the registration.

Myocardium Segmentation to Define the Incompressible Region For each image sequence we used an interactive 3D segmentation tool that builds a 3D mask image and mesh. Control points are added by the user to define the inside, outside, and border of the region, from which a 3D mesh is constructed using an implicit variational surfaces approach. The tool is included within the CardioViz3D software package available for download[3]. For further details on the tool see [7]. We segmented the LV endocardium and the LV epicardium and then applied arithmetic tools to obtain the LV myocardium image. We then dilate the resulting mask to ensure that the full myocardium is covered and to avoid possible boundary effects. The incompressibility domain is shown in yellow for each of the the imaging modalities (see Fig. 1). A screenshot of the segmentation tool is shown in Fig. 2.

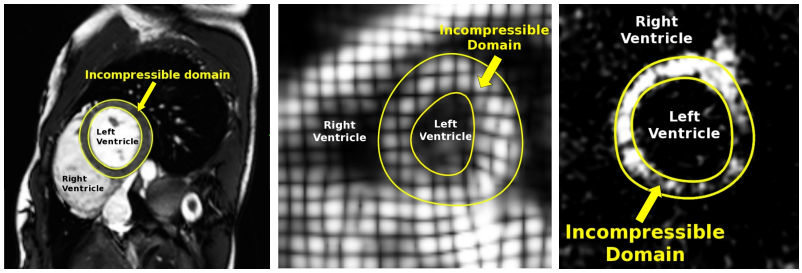

Fig. 1: The incompressibility domain shown on a cine-MR image (left), tagged-MR image (center) and echocardiography image (right). This domain defines where the incompressibility constraint is enforced in the registration algorithm.

[3] *http://www-sop.inria.fr/asclepios/software/CardioViz3D/*

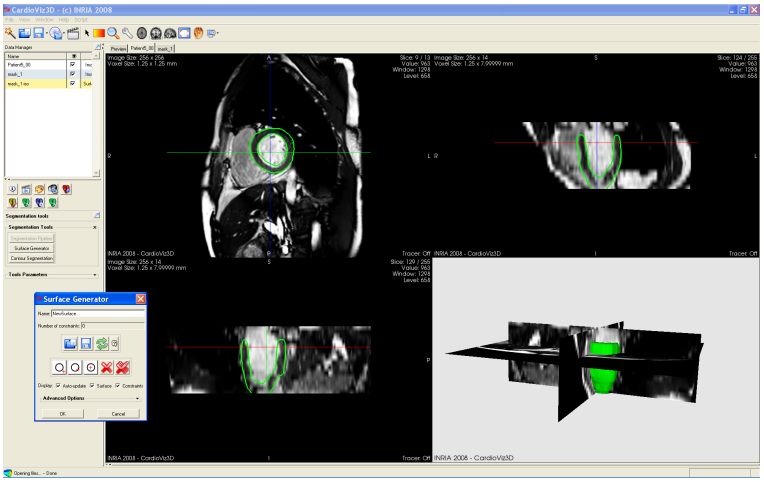

Fig. 2: A screenshot of the interactive segmentation tool in CardioViz3D which can be downloaded from *http://www-sop.inria.fr/asclepios/software/CardioViz3D/*. The tool requires the user to place control points, from which a surface is build using implicit variational surfaces approach.

Isotropic Resampling The cine-MR images have anisotropic voxel sizes. To correct for this, we re-sampled the voxels to be isotropic in all directions. Isotropic voxel size improves the registration since the transformation is defined on a grid with enough resolution to avoid "aliasing" effects (as is true for any demons algorithm). The echocardiography and tagged-MR image sequences had already isotropic voxels.

Contrast enhancement To enhance the image contrast we clamped the tails of the grey-level histogram to exclude the 1st and 99th quantiles. The grey level intensities were then normalized for each slice using a fixed scale. This was done for each image in the sequence independently. An example of the before and after image is shown in Fig 3. This processing also reduced the effects of tag fading, thus further improving registration results.

4 Application to Challenge Data

The algorithm was applied to a data-set of 15 volunteers and one phantom, each with cine-MR, tagged-MR and echocardiography images. The resulting deformation fields for each modality are included in the motion tracking challenge. To demonstrate the performance of this method we show the results for each modality for one patient from the data-set of 15 volunteers as well as the results for the phantom data. Similar results were obtained for the remaining volunteers.

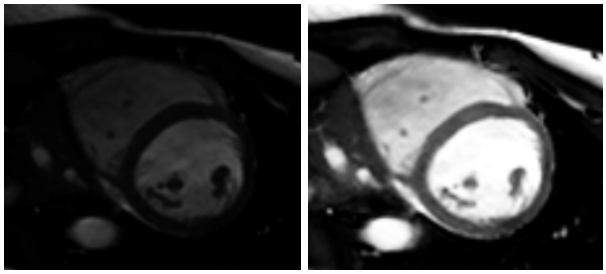

Fig. 3: Original image (left) and processed image (right) after histogram clamping and normalization to improve image contrast.

4.1 Results for Echocardiography Sequences

The method was first applied to echocardiography image sequences. In this case, the images show well the endocardium (inside the heart) but the epicardium is difficult to see, particularly in the free wall. However, the motion is more apparent in the echocardiography sequences than in cine-MR due to the speckle that is "stitched" to the muscle and thus follows it as the heart deforms, though this speckle is consistent only between few time frames. Figure 4 (first two rows) shows one patient image at full contraction (systole) with the mask propagated using the deformation field computed in the registration overlaid on the image and similarly for the phantom. The masked deformation field is shown on the patient and phantom at full contraction to illustrate the direction and magnitude of motion. In each case the registration captures the expected longitudinal contraction, and circumferential twisting of the ventricle. We can also observe that, although it is difficult to distinguish clearly the epicardium for this modality, the algorithm is able to produce reasonable strain curves, as shown in Fig 5.

4.2 Results for Cine-MR Image Sequences

The algorithm was applied to the short-axis cine-MR images. These images show clearly the myocardium, though there is little information in the apex due to too few slices in the through plane. The algorithm is able to capture a realistic motion of the myocardium, as shown in the middle two rows of Fig 4. The strain curves for cine-MR are under-estimated mainly due to lack of texture information in the images but show the expected trends (increase in strain towards peak systole, followed by decrease at rest (see Fig 5).

4.3 Results for Tagged-MR Image Sequences

As expected, the tagged-MR registration captures the twisting motion of the myocardium very well, this is particularly evident in the phantom (see Fig 4 bottom row second to the right), as well as the longitudinal contraction. The strain curves for the tagged-MR data shown in Fig 5 show a reasonable trend, however the standard deviation over the given regions is high in this case.

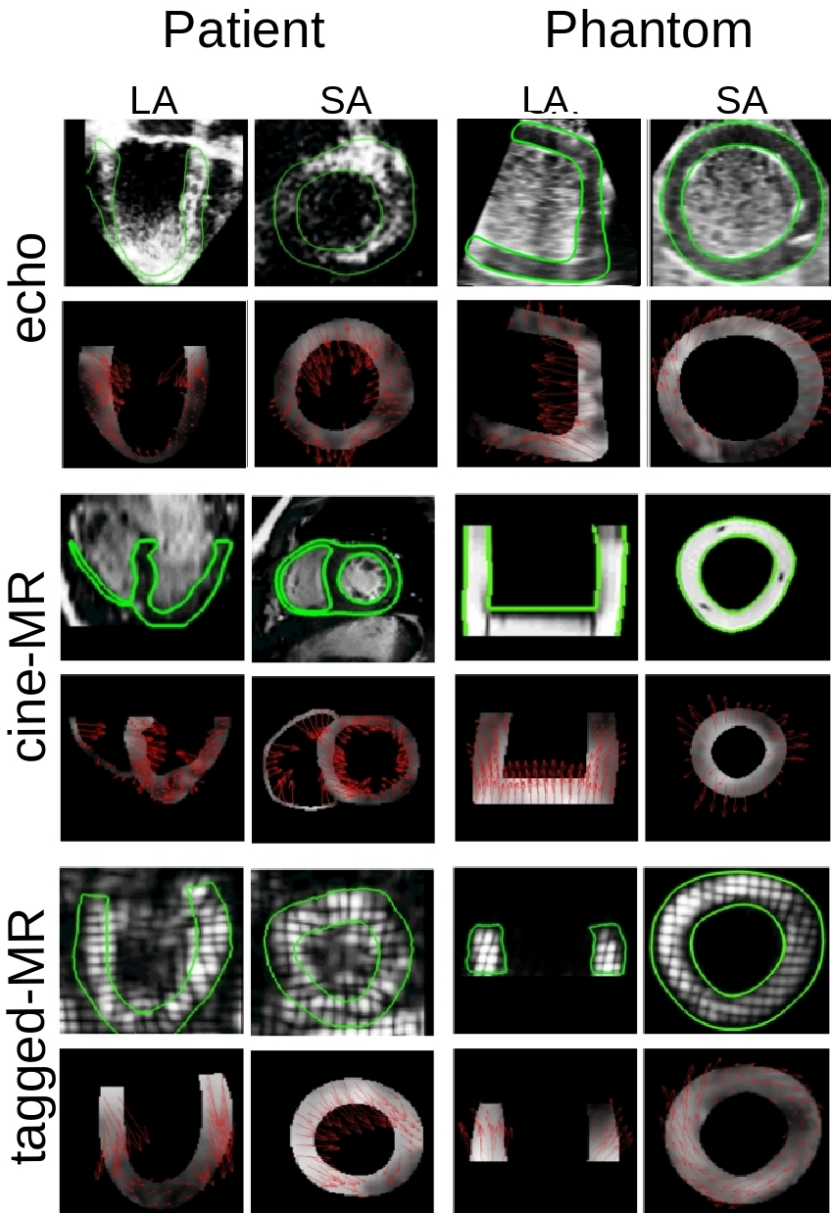

Fig. 4: Top row: Long axis and short axis views of echocardiography images for one patient (left two columns) and the phantom (right two columns) shown at full contraction overlaid with the mask deformed by the deformation computed using iLogDemons. Second row: Two views of the computed deformation field (normal of intensities and vectors) shown only in the mask region for one patient image (left columns) and the phantom (right columns). Similarly for cine-MR (third and fourth rows) and tagged-MR (fifth and sixth rows). For each modality a realistic motion is obtained (rows one, three and five), as well as the desired direction and magnitude of motion (rows two, four and six), particularly for the phantom. In particular, the longitudinal motion captured by the algorithm can be seen by the vectors pointing downwards towards the apex in the long axis views of rows two, four and six, and the circumferential motion can be seen in the short axis views where the vectors appear to be wrapping around the muscle to an extent.

5 Strain Estimation

The strain curves in each of the 17 AHA regions in each of the radial, circumferential and longitudinal directions were computed for each of the modalities. The strain was computed using the 3D Lagrangian finite strain tensor

$$E(x) = \frac{1}{2}[\nabla \mathbf{u}(x) + \nabla \mathbf{u}^T(x) + \nabla \mathbf{u}^T(x)\nabla \mathbf{u}(x)] \tag{4}$$

for the estimated displacement $\mathbf{u}(x)$ from the iLogDemons registration at the spatial positions x. The computed strain tensors were then projected onto a local prolate coordinate system as described in [1].

The strain curves for each modality in each direction are shown in Fig 5. The curves show a good consistency between the modalities in respect to curve trends, with the strain rising to a peak in the middle of the cycle at peak systole, and decreasing back towards zero (note that the curves are not temporally synchronized). The curves for the echocardiography sequence show a good agreement to those previously found for cine-MR and tagged-MR presented in [1]. However, the curves for the cine-MR sequence show less consistency with previously published results in [8], as they are under-estimated in all directions. Possible reasons for this could be too much smoothing, a lack of texture information, poor image resolution or errors in the tracking. The curves of the standard deviation among the zones shown are similar to the mean curves shown in green, which displays the consistency among the AHA regions which is expected in healthy subjects with synchronized movement among the regions. Note that here we exclude the apical regions since the apex is not clearly visible in all images.

6 Discussion

In general, this method provides reasonable results for tracking the myocardium in the three modalities. In particular, the method gives good results for the echocardiography sequences for both the tracking and estimation of strain even given data with poor visibility and little structural information. The method is particularly useful for cardiac motion tracking due to the fact that it can be applied to the imaging modalities that are most commonly used in cardiology.

6.1 Incompressibility constraint

We discuss here the advantages and disadvantages of enforcing the incompressibility constraint in the myocardium. The constraint was integrated into the LogDemons method initially to be used on cine-MR sequences, which are known to exhibit only apparent motion in the image. For this reason, it seemed natural to constrain the myocardium to be incompressible to reduce the number of unknowns to force a circumferential and longitudinal deformation when there is a radial contraction/expansion. In the case of echocardiography sequences and tagged-MR sequences, there is more texture information in the image that

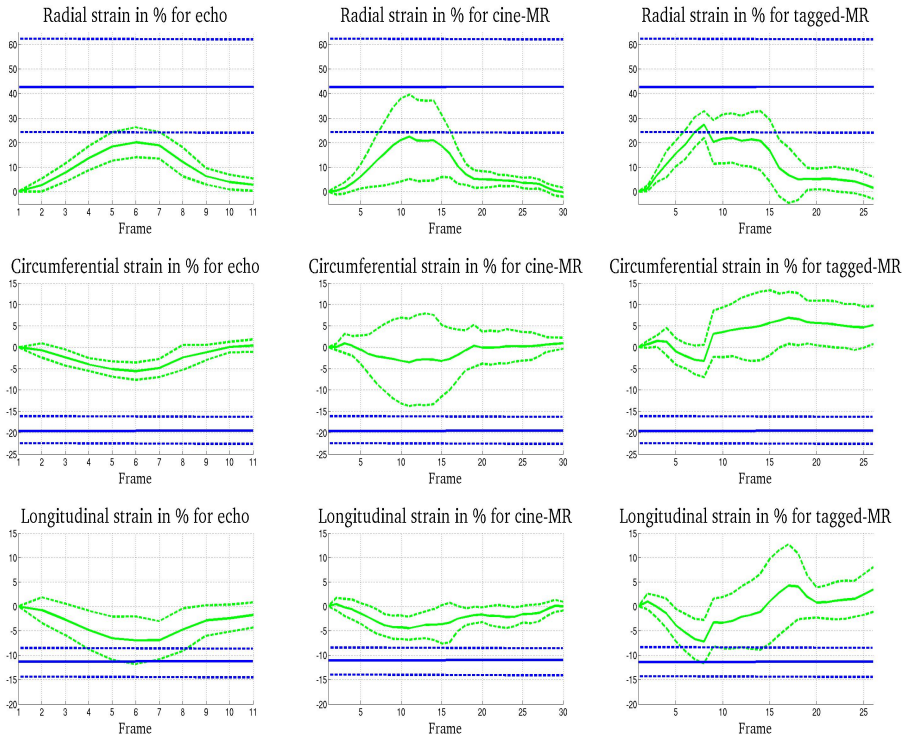

Fig. 5: Strain curves in the radial (left), circumferential (middle) and longitudinal (right) directions for echocardiography sequence (top row), cine-MR sequence (middle row) and tagged-MR sequence (bottom row) for one subject. Mean (solid line) and standard deviation (dashed line) are shown for one patient in green, and the mean and standard deviations for systolic strain reported in [8] are shown in blue. Note that the curves have not been temporally synchronized. We can see that the magnitudes are under-estimated, though the curve trends are consistent with what is expected with a peak strain at peak contraction in the radial direction, minimum strain at peak contraction for circumferential and longitudinal strain.

aids in capturing this motion (speckles in echocardiography images, tag grids in tagged-MR). Nonetheless, for the purposes of the challenge we applied the method to all modalities to analyse the results.

Myocardium Segmentation Since the method requires a mask of the myocardium, we segmented these prior to running the algorithm using the tool described in Section 3. The incompressibility constraint relies heavily on the accuracy of the segmentation, therefore errors in the tracking can arise due to mis-segmentation of the tissue. This is a problem in particular for the echocardiography and tagged-MR images, which are known to be hard to segment given the poor image quality, poor visibility of the myocardium and noise from the top of the cone in echo images. However, this is the case for any method using localized incompressibility

constraint to track the myocardium. In this work, we used a binary mask for the myocardium. To avoid possible problems related to the boundary conditions, we dilated the mask by 2 voxels.

Constrained incompressibility vs. compressibility A common point of discussion for constraining the myocardium to be incompressible is that the myocardium is not in fact fully incompressible. In the literature, the myocardium is observed to have a volume change of around 5% [9]. In the case of the LogDemons algorithm, there is no constraint on the compressibility of the myocardium, which results in up to 30% volume change, compared to less than 7% of numerical volume change for the iLogDemons algorithm (see Fig 6). Therefore, while the iLogDemons algorithm may under-estimate the volume change in general, with the unconstrained LogDemons algorithm it can be greatly-overestimated. Furthermore, improved strain curves were obtained in [1] compared to those computed from the LogDemons algorithm. Hence, the incompressibility constraint is a useful prior for cardiac motion tracking, though penalising rather than constraining the compressibility may be more physiologically realistic.

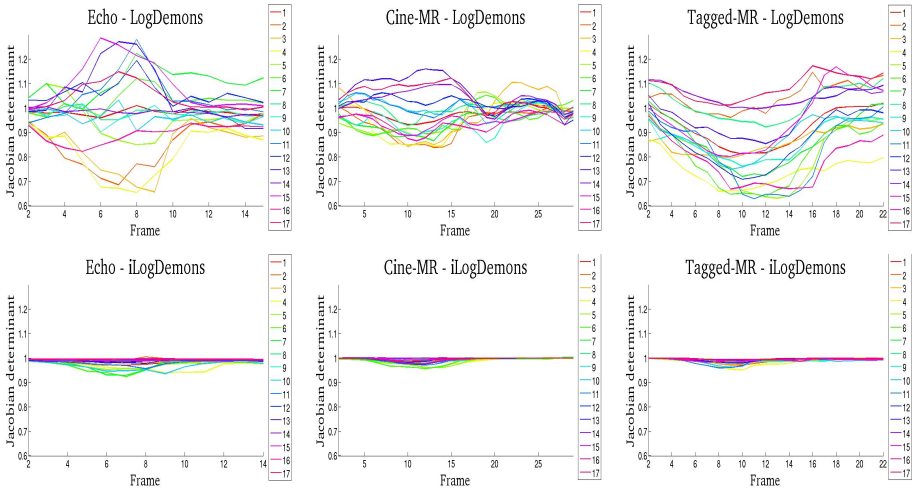

Fig. 6: Average jacobian determinant in each of the 17 AHA regions for the LogDemons algorithm (top row) and iLogDemons (bottom row) for each of the modalities (echo-left column, cine-MR - centre column, tagged-MR - right column). The iLogDemons algorithm constrains the compressibility to be less than 7% for each modality compared to up to 30% compressibility for LogDemons.

6.2 Field of View

In some of the sequences in the challenge data-set, the myocardium was on or very close to the border of the image, particularly in the tagged-MR sequences

which have a very narrow field of view. How the image and the deformation are treated at the boundary of the image (extrapolated to invisible data) is a key problem in most registration algorithms. Currently the iLogDemons algorithm works in such a way that the intensities on the border of the image are extrapolated outside the image in a given region.

7 Conclusion

The iLogDemons algorithm was applied to a data-set of 15 subjects and one phantom each with an echocardiography, cine-MR and tagged-MR image sequence. This method was developed for the heart to model elasticity of the tissue and incompressibility in the myocardium. The results show that given few changes in the input parameters, the method is able to retrieve realistic motion of the heart as well as reasonable strain curves for each of the three modalities and is thus a versatile registration algorithm for cardiac motion tracking. However, future work is needed to further analyse the incompressibility prior, possibly including a change in the way the prior is incorporated into the model by means of a penalisation of the compressibility rather than the current method of constraining the velocity fields to be divergence-free.

Acknowledgements: This project was partially funded by the Care4Me ITEA2 project.

References

1. Mansi, T., Pennec, X., Sermesant, M., Delingette, H., Ayache, N.: ilogdemons: A demons-based registration algorithm for tracking incompressible elastic biological tissues. Int. J. of Computer Vision (2011)
2. Vercauteren, T., Pennec, X., Perchant, A., Ayache, N.: Symmetric log-domain diffeomorphic registration: A demons-based approach. In: Proc. of MICCAI'08, Part I. Volume 5241 of LNCS., Springer (2008) 754–761
3. Arsigny, V., Commowick, O., Pennec, X., Ayache, N.: A log-euclidean framework for statistics on diffeomorphisms. In: Proc. of MICCAI'06, Part I. Volume 4791 of LNCS., Springer (2006) 924–931
4. Dru, F., Vercauteren, T.: An ITK implementation of the symmetric log-domain diffeomorphic demons algorithm. Insight Journal - 2009 January - June (2009)
5. Simard, P.Y., Mailloux, G.E.: A projection operator for the restoration of divergence-free vector fields. IEEE Transaction on Pattern Analysis and Machine Intelligence **10** (1988) 248–256
6. Saad, Y.: Iterative methods for sparse linear systems. Volume 73 of Society for Industrial Mathematics. PWS (2003)
7. Mansi, T.: Image-Based Physiological and Statistical Models of the Heart, Application to Tetralogy of Fallot. Thèse de sciences (phd thesis), Ecole Nationale Supérieure des Mines de Paris (September 2010)
8. Moore, C., Lugo-Olivieri, C., McVeigh, E., Zerhouni, E.: Three-dimensional systolic strain patterns in the normal human left ventricle: Characterization with tagged MR imaging. Radiology **214** (2000) 453–466
9. Glass, L., Hunter, P., McCulloch, A.: Theory of Heart: Biomechanics, Biophysics, and Nonlinear Dynamics of Cardiac Function. Springer-Verlag (1991)